

Skyrmion-electron bound states in a Néel antiferromagnet

N. Davier^{1,*} and R. Ramazashvili^{1,†}

¹*Laboratoire de Physique Théorique, Université de Toulouse, CNRS, UPS, France*

(Dated: March 8, 2022)

We show that, in a Néel antiferromagnet with a particular location of electron band extrema, a Skyrmion and an electron form a bound state with energy of the order of the gap Δ in the electron spectrum. The bound state turns the Skyrmion into a charged particle, that may be manipulated by electric field. We identify a region in the space of coupling constants, where the Skyrmion-electron bound state makes the (otherwise metastable) Skyrmion genuinely stable.

Introduction — Over the past years, spintronics has been undergoing explosive growth, engaging ever new areas of research. Physics of domain walls, Skyrmions and other topologically protected magnetic textures has become one such area, that brought together fundamental and applied science, from novel states of matter such as Skyrmion lattice to memory devices that use Skyrmions and domain walls to process information [1]. In this context, antiferromagnetic Skyrmions have been attracting much attention [2], especially in view of the promise they are seen to hold for devices. Yet a single Skyrmion is metastable, and controllably generating a sufficiently long-lived Skyrmion in an antiferromagnet remains a challenge, requiring a fine balance of numerous factors including competing exchange couplings, Dzyaloshinskii-Moriya (DM) interaction, single-ion anisotropy, temperature, and magnetic field [3]. To stabilize different Skyrmion configurations, various setups have been proposed, such as those with an antiferromagnetically ordered substrate producing an effective staggered magnetic field [4], or those with a conducting substrate generating the Ruderman-Kittel-Kasuya-Yosida interaction [5].

Here we study a Skyrmion in an antiferromagnetic insulator, doped by a single electron, and demonstrate a hitherto unexplored mechanism that enhances the Skyrmion stability: We show that, for a specific location of the electron band extrema in the Brillouin zone, the Skyrmion binds the electron and becomes charged. The bound-state energy has the scale of the antiferromagnetic gap Δ in the electron spectrum, and depends on the Skyrmion profile. The resulting profile is defined by interplay of the bound-state energy with magnetic couplings such as exchange, single-ion anisotropy and DM interaction. We identify a region in the space of coupling constants, where the bound state renders the (otherwise metastable) Skyrmion truly stable. Together with the appearance of the Skyrmion-electron bound state, this is the main result of our work.

A tractable example is provided by a perfectly isotropic centrosymmetric antiferromagnet, where the Skyrmion assumes the Belavin-Polyakov (BP) form [6] parameterized by a single length: the radius R . In the absence of an electron, the energy of the BP Skyrmion is indepen-

dent of R . By contrast, below we show that the electron bound state energy $\epsilon(R)$ has a minimum at an $R = R^*$ of the order of the antiferromagnetic ‘coherence length’ $\xi = \frac{\hbar v}{\Delta}$, with v the Fermi velocity of the parent paramagnetic state. This minimum $|\epsilon(R^*)| \sim \Delta$ defines the ensuing BP Skyrmion size of the order of ξ .

We begin with deriving the low-energy Hamiltonian of a single electron in a centrosymmetric Néel antiferromagnet in the presence of a smooth texture. Then we focus on a square-lattice antiferromagnet with a specific location of the electron band extrema, and a single BP Skyrmion. We show that the Skyrmion binds the electron, and study evolution of the bound state as a function of the Skyrmion size. Finally, we discuss the validity range of our results and their broader implications.

Effective Hamiltonian — Consider a collinear Néel antiferromagnet on a square-symmetry lattice with period a . Its ordered moment changes sign upon elementary translation, and couples electron states at any two momenta \mathbf{p} and $\mathbf{p} + \mathbf{Q}$, separated by the Néel wave vector $\mathbf{Q} = (\pm \frac{\pi}{a}, \pm \frac{\pi}{a})$. The coupling has the form of exchange $(\Delta \cdot \sigma)$, with Δ proportional to the staggered magnetization, and σ the triad of Pauli matrices, representing electron spin. Since \mathbf{p} and $\mathbf{p} + 2\mathbf{Q}$ are equivalent, the Hamiltonian \mathcal{H} acts on a bispinor $\Psi = (\psi_{\mathbf{p}}, \psi_{\mathbf{p}+\mathbf{Q}})$ and, for a uniform Δ , reads [7]

$$\mathcal{H} = \begin{bmatrix} \varepsilon(\mathbf{p}) & (\Delta \cdot \sigma) \\ (\Delta \cdot \sigma) & \varepsilon(\mathbf{p} + \mathbf{Q}) \end{bmatrix}, \quad (1)$$

where $\varepsilon(\mathbf{p})$ is the electron dispersion in the absence of Néel order. The resulting spectrum $E_{\mathbf{p}} = \varepsilon_{\pm}(\mathbf{p}) \pm \sqrt{|\Delta|^2 + \varepsilon_{\pm}^2(\mathbf{p})}$, where $\varepsilon_{\pm}(\mathbf{p}) \equiv \frac{1}{2}[\varepsilon(\mathbf{p}) \pm \varepsilon(\mathbf{p} + \mathbf{Q})]$, is doubly degenerate and has a gap $\Delta = |\Delta|$, which turns a half-filled metal into an insulator.

In the presence of a smooth texture $\Delta_{\mathbf{r}} = \hat{\mathbf{n}}_{\mathbf{r}}\Delta$, with unit vector $\hat{\mathbf{n}}_{\mathbf{r}}$ dependent on the coordinate \mathbf{r} , carriers near the extrema of $E_{\mathbf{p}}$ at momenta \mathbf{p}_0 and $\mathbf{p}_0 + \mathbf{Q}$ admit an effective-mass Hamiltonian description [8]. To derive it, in Eq. (1) we replace uniform Δ by $\Delta_{\mathbf{r}}$, and substitute $\hat{\mathbf{p}} \equiv -i\hbar\nabla$ for the momentum dependences $\varepsilon_{\mathbf{p}_0}(\hat{\mathbf{p}})$ and $\varepsilon_{\mathbf{p}_0+\mathbf{Q}}(\hat{\mathbf{p}})$ of $\varepsilon(\mathbf{p})$ near \mathbf{p}_0 and $\mathbf{p}_0 + \mathbf{Q}$.

Then we perform a spin rotation $U_{\mathbf{r}}$ that makes $\Delta_{\mathbf{r}}$ uniform: $U_{\mathbf{r}}^{\dagger}(\hat{\mathbf{n}}_{\mathbf{r}} \cdot \sigma)U_{\mathbf{r}} = \sigma_z$ [9]. This generates a Peierls

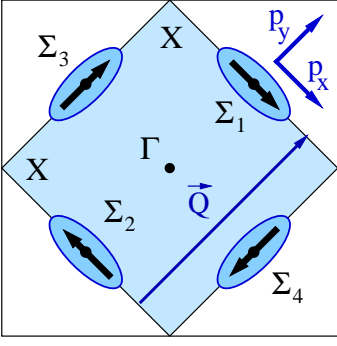


FIG. 1: The Brillouin zone of a square-lattice Néel anti-ferromagnet with wave vector $\hat{\mathbf{Q}} = (\pm\frac{\pi}{a}, \pm\frac{\pi}{a})$. The large square shows the Brillouin zone in the paramagnetic state, the shaded smaller square depicts the Brillouin zone in the Néel state (MBZ). The band extrema are assumed to lie at face centers Σ_1 - Σ_4 of the MBZ. The p_x, p_y are the local momentum axes near Σ_1 , as used in the main text. The ellipses are the equal- $E_{\mathbf{p}}$ lines near Σ_1 - Σ_4 . The bold arrows centered at Σ_1 - Σ_4 show the electron spin polarization of the bound state in each valley, for a large BP Skyrmion of Néel type (see main text for details).

substitution $\hat{p}_i \rightarrow \hat{p}_i + (\mathbf{A}_i \cdot \boldsymbol{\sigma})$ in $\varepsilon_{\mathbf{p}_0}(\hat{\mathbf{p}})$ and $\varepsilon_{\mathbf{p}_0+\mathbf{Q}}(\hat{\mathbf{p}})$, with $(\mathbf{A}_i \cdot \boldsymbol{\sigma}) = A_i^\alpha \sigma^\alpha = -i\hbar U_{\mathbf{r}}^\dagger \partial_i U_{\mathbf{r}}$. Vector potential A_i^α carries real-space indices $i = x, y$ and spin indices $\alpha = x, y, z$. While different components of $(\mathbf{A} \cdot \boldsymbol{\sigma})$ do not commute, $U_{\mathbf{r}}$ is defined only up to a non-uniform spin rotation $V_{\mathbf{r}}^z = e^{i\sigma_z \chi}$ around \hat{z} : $U_{\mathbf{r}} \rightarrow U_{\mathbf{r}} V_{\mathbf{r}}^z$, which is an abelian transformation. This gauge transformation acts on $(\mathbf{A} \cdot \boldsymbol{\sigma})$ in a peculiar way, elucidated by first-order expansion in infinitesimal χ :

$$\delta(\mathbf{A}_i \cdot \boldsymbol{\sigma}) = \sigma^z \partial_i \chi + \chi [(\mathbf{A}_i \cdot \boldsymbol{\sigma}), \sigma_z]. \quad (2)$$

That is, A_i^z transforms as electromagnetic vector potential ($\delta A_i^z = \partial_i \chi$), while $\mathbf{A}_i^\parallel = (A_i^x, A_i^y)$ rotates around \hat{z} by angle 2χ . This observation will prove useful below.

The next step involves splitting the bispinor Ψ into two spin- $\frac{1}{2}$ components, for energies near $\pm\Delta$, akin to taking the Dirac Hamiltonian to its non-relativistic Pauli-Schrödinger limit [10, 11]. Hereafter, we focus on the conduction band (energies E near $+\Delta$) and, to first order in $\frac{E-\Delta}{\Delta}$, find the effective low-energy Hamiltonian $\mathcal{H}_{\mathbf{p}_0}$ near \mathbf{p}_0 , with $\bar{\varepsilon}_{\mathbf{p}_0+\mathbf{Q}}(\hat{\mathbf{p}}) \equiv \sigma_z \varepsilon_{\mathbf{p}_0+\mathbf{Q}}(\hat{\mathbf{p}}) \sigma_z$:

$$\mathcal{H}_{\mathbf{p}_0} = \frac{\varepsilon_{\mathbf{p}_0}(\hat{\mathbf{p}}) + \bar{\varepsilon}_{\mathbf{p}_0+\mathbf{Q}}(\hat{\mathbf{p}})}{2} + \frac{[\varepsilon_{\mathbf{p}_0}(\hat{\mathbf{p}}) - \bar{\varepsilon}_{\mathbf{p}_0+\mathbf{Q}}(\hat{\mathbf{p}})]^2}{8\Delta}. \quad (3)$$

The explicit form of Hamiltonian (3) depends on that of $\varepsilon_{\mathbf{p}_0}(\hat{\mathbf{p}})$ and $\varepsilon_{\mathbf{p}_0+\mathbf{Q}}(\hat{\mathbf{p}})$, in its turn set by the symmetry of momenta \mathbf{p}_0 and $\mathbf{p}_0 + \mathbf{Q}$ in the Brillouin zone. Here we focus on the extrema at midpoints Σ of the magnetic Brillouin zone (MBZ) boundary in Fig. 1. The momentum expansion of $\varepsilon_{\mathbf{p}_0}(\hat{\mathbf{p}})$ and $\varepsilon_{\mathbf{p}_0+\mathbf{Q}}(\hat{\mathbf{p}})$ begins with $\pm \mathbf{v} \cdot \hat{\mathbf{p}} + \hat{p}_i^2/2m_i$, with the paramagnetic-state Fermi velocity \mathbf{v} at Σ pointing along the local p_y in Fig. 1, and

$m_i = m_x, m_y$ the paramagnetic-state effective masses along and normal to the MBZ boundary. Truncating the momentum expansion of Eq. (3) at quadratic terms [12], we find

$$\mathcal{H}_{\Sigma} = \frac{(\hat{p}_i + A_i^z \sigma_z)^2}{2m_i^*} + \frac{(A_i^\parallel)^2}{2m_i} + v (\mathbf{A}_y^\parallel \cdot \boldsymbol{\sigma}). \quad (4)$$

Despite its peculiar appearance, Hamiltonian (4) is gauge-invariant: recall that, by Eq. (2), gauge transformation of \mathbf{A}_i^\parallel amounts to its spin rotation around \hat{z} . Hamiltonian (4) is an extension, to non-planar textures, of the approach used to study planar spiral phases in doped antiferromagnets [13].

Note that m_y^* in Eq. (4) is renormalized relative to m_y in the expansion of $\varepsilon_{\mathbf{p}_0}(\hat{\mathbf{p}})$ and $\varepsilon_{\mathbf{p}_0+\mathbf{Q}}(\hat{\mathbf{p}})$, as per $(m_y^*)^{-1} = (m_y)^{-1} + \frac{v^2}{\Delta}$. Thus, m_y^* tends to be tiny compared with m_y : $\frac{m_y^*}{m_y} \sim \frac{\Delta}{\epsilon_F} \ll 1$, while $m_x^* = m_x$ is of the order of band electron mass m or greater: observe that, with only the nearest-neighbor hopping, m_x at Σ is infinite. Such a mass anisotropy arises for *any* (not only Néel) $(\frac{\pi}{a}, \frac{\pi}{a})$ order with a gap $\Delta \ll \epsilon_F \equiv mv^2$. Electron-doped cuprates at low-to-optimal doping provide a prominent example [14–16], even if the nature of their ordering remains controversial, with experimental evidence presented both against [17–20] and for [21–26] the presence of (quasi)static Néel order.

Belavin-Polyakov Skyrmion — Let us turn to a specific texture: a single Skyrmion in a centrosymmetric isotropic Néel antiferromagnet. Its continuum-limit energy density is $J(\nabla \hat{\mathbf{n}}_{\mathbf{r}})^2$, with stiffness J . Under condition defined below, the Skyrmion profile $\hat{\mathbf{n}}_{\mathbf{r}} = (\sin \theta \cos \phi, \sin \theta \sin \phi, \cos \theta)$ can be used as static input to the electron problem. In the topological sector with winding number \mathcal{Q} , the lowest-energy solution is the BP Skyrmion of radius R and R -independent energy $4\pi J \mathcal{Q}$ [6]. Thus, as a toy problem, we study a single electron in the presence of a $\mathcal{Q} = 1$ BP Skyrmion. We focus on a high-symmetry configuration, with the polar angle θ of $\hat{\mathbf{n}}_{\mathbf{r}}$ dependent only on the distance $r = \sqrt{x^2 + y^2}$ to the Skyrmion center, and $\phi = \arctan \frac{y}{x}$ the azimuthal angle in the (x, y) plane. The energy density above is invariant under shifting ϕ by a constant γ , usually called ‘helicity’ [2]. This allows us to reduce the problem to the $\gamma = 0$ pattern, commonly called the ‘Néel’ Skyrmion.

To proceed, we fix the gauge by choosing $U_{\mathbf{r}} = (\mathbf{m}_{\mathbf{r}} \cdot \boldsymbol{\sigma})$, with $\mathbf{m}_{\mathbf{r}}$ pointing along the bisector between \hat{z} and $\Delta_{\mathbf{r}}$. Such a $U_{\mathbf{r}}$ rotates $\Delta_{\mathbf{r}}$ around $\mathbf{m}_{\mathbf{r}}$ by angle π , and brings $\Delta_{\mathbf{r}}$ to point along \hat{z} [27].

Let us turn to Hamiltonian (4). The BP Skyrmion of radius R is defined by $\sin \theta = \frac{2z}{1+z^2}$ with $z = \frac{r}{R}$, so that $\theta[R] = \frac{\pi}{2}$. As a result, the spin- z components A_i^z in the first term of Eq. (4) read

$$A_x^z = \frac{-\hbar y}{R^2 + r^2}, \quad A_y^z = \frac{\hbar x}{R^2 + r^2}. \quad (5)$$

Thus, the Skyrmion produces geometric flux $\pm 2\pi\hbar$ for the spin-up and spin-down components of the wave function: $\oint A_i^z dl_i = 2\pi\hbar$, with the integral taken along a circle, large against R [28]. This causes the spin Hall effect. The second term in Eq. (4) creates a repulsive potential

$$\frac{(A_i^{\parallel})^2}{2m_i} = \frac{\hbar^2}{2R^2} \left[\frac{1}{m_x} + \frac{1}{m_y} \right] \frac{1}{(1+z^2)^2}, \quad (6)$$

whereas the last term takes the form

$$v(\mathbf{A}_y^{\parallel} \cdot \boldsymbol{\sigma}) = -\frac{\hbar v}{R} \frac{\sigma^x}{1+z^2}, \quad (7)$$

and thus produces an attractive potential for the spin-up component of the wave function along the \hat{x} axis [29]. Direct inspection shows that, for $R \gg \xi = \frac{\hbar v}{\Delta}$, the r.h.s. of Eq. (7) overwhelms all the other terms with A_i^α in Eq. (4), and creates a Skyrmion-electron bound state, the key result of our work. The bound state is nondegenerate and, at $R \gg \xi$, spin-polarized in each of the four Σ valleys as shown in Fig. 1 [30].

The mass anisotropy $\frac{m_y^*}{m_x^*} \sim \frac{\Delta}{\epsilon_F} \ll 1$ of Hamiltonian (4) makes the y coordinate ‘fast’ relative to x , and the bound-state energy can be readily evaluated using the Born-Oppenheimer approximation [31]. For $R \gg \xi$, the energy ϵ_0^c of the lowest bound state, generated by the conduction band, can be evaluated by expanding the r.h.s. of (7) to first order in z^2 and finding the ground state of the ensuing harmonic oscillator with respect to y :

$$\epsilon_0^c(R) \approx -\Delta \frac{\xi}{R} \left[1 - \frac{1}{2^{3/2}} \sqrt{\frac{\xi}{R}} \right]. \quad (8)$$

Subsequent account of the ‘slow’ coordinate x introduces only a correction of the order of $\sqrt{\frac{a}{\xi}} \ll 1$ to the coefficient $2^{-3/2}$ in Eq. (8). For $R \gg \xi$, the bound state (8) is shallow ($|\epsilon_0^c| \ll \Delta$), and the low-energy approximation of Hamiltonians (3) and (4) remains valid. However, with R decreasing, $|\epsilon_0^c|$ grows to attain the order of Δ at $R \sim \xi$, where the low-energy approximation breaks down along with Hamiltonians (3) and (4), as sketched in Fig. 2.

Now we will show that, with R decreasing further below ξ , the bound state becomes shallow again, and vanishes at an $\bar{R} \sim \sqrt{\frac{m_y}{m_x}} \sqrt{\xi a}$. To make this length scale manifest, we eliminate A_y^z from the first term in Eq. (4) by gauge transformation

$$W = e^{i\sigma_z \chi}, \quad \chi(\tilde{x}, \tilde{y}) = \frac{-\tilde{x}}{\sqrt{1+\tilde{x}^2}} \arctan \frac{\tilde{y}}{\sqrt{1+\tilde{x}^2}}, \quad (9)$$

where $\tilde{x} = \frac{x}{\bar{R}}$ and $\tilde{y} = \frac{y}{\bar{R}}$. As a result, Hamiltonian (4) takes the form

$$\tilde{\mathcal{H}}_\Sigma = \frac{\hat{p}_y^2}{2m_y^*} + v(\tilde{\mathbf{A}}_y^{\parallel} \cdot \boldsymbol{\sigma}) + \frac{(A_i^{\parallel})^2}{2m_i} + \frac{(\hat{p}_x + \tilde{A}_x^z \sigma_z)^2}{2m_x}, \quad (10)$$

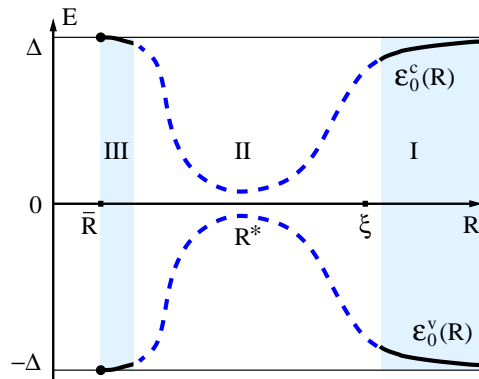


FIG. 2: Energy $\epsilon_0^c(R)$ of BP Skyrmion-electron bound state, generated by the conduction band, and of its valence-band counterpart $\epsilon_0^v(R)$, sketched as a function of the BP Skyrmion radius R . **In region I** ($R \gg \xi = \frac{\hbar v}{\Delta}$), the bound state is described by low-energy Hamiltonian (4). The $\epsilon_0^c(R)$ is given by Eq. (8) and shown by solid line. **In region II** ($\bar{R} \ll R \lesssim \xi$), the low-energy approximation breaks down, and the bound state (dashed line) must be found from the full Hamiltonian of a kind (1) in the presence of the Skyrmion, which goes beyond the scope of this work. At an $R^* \lesssim \xi$, the $\epsilon_0^c(R)$ has a minimum that defines the ‘optimal’ Skyrmion size. **In region III** (narrow range $R - \bar{R} \ll \bar{R}$), the bound state, shown by solid line, becomes shallow again, and disappears at $R = \bar{R}$ (see main text).

where $\tilde{A}_x^z = A_x^z + \partial_x \chi$, and

$$(\tilde{\mathbf{A}}_y^{\parallel} \cdot \boldsymbol{\sigma}) = A_y^{\parallel} [\sigma^x \cos 2\chi + \sigma^y \sin 2\chi].$$

In terms of the ‘fast’ coordinate y , Hamiltonian (10) describes a particle in a one-dimensional potential $\mathcal{U}_x(y)$, parametrically dependent on the ‘slow’ variable x , which again invites the Born-Oppenheimer approximation. Comparing the characteristic value $\frac{\hbar v}{R}$ of the second term in Eq. (10) with typical kinetic energy $\frac{\hbar^2}{m_y^* R^2}$ of the trapped electron, we find that the former is indeed small against the latter for $R \ll \xi$, the range in question. The effective bound-state energy is thus defined by the integrated potential $u(x) = \int \mathcal{U}_x(y) dy$ [32]. Contribution of the second term in Eq. (10) to $u(x)$ is

$$u_1(x) \sigma^x = -v \int dy (\tilde{\mathbf{A}}_y^{\parallel} \cdot \boldsymbol{\sigma}) = \hbar v \sigma^x \frac{\sin\left(\frac{\pi \tilde{x}}{\sqrt{1+\tilde{x}^2}}\right)}{\tilde{x}}. \quad (11)$$

The third term in Eq. (10) is an $\frac{a}{R} \ll 1$ fraction of the second, thus its contribution to $u(x)$ can be neglected as long as continuum description of the Skyrmion applies ($R \gg a$). By contrast,

$$u_2(x) = \frac{1}{2m_x} \int dy (\tilde{A}_x^z)^2, \quad (12)$$

arising from the last term, requires care since $(\tilde{A}_x^z)^2$ re-

mains finite as $y \rightarrow \infty$:

$$A^2(x) \equiv \lim_{y \rightarrow \infty} (\tilde{A}_x^z)^2 = \frac{\hbar^2}{R^2} \frac{[\pi/2]^2}{(1 + \tilde{x}^2)^3},$$

which makes $u_2(x)$ diverge. We remedy this by writing $(\tilde{A}_x^z)^2 = [(\tilde{A}_x^z)^2 - A^2(x)] + A^2(x)$. The term in the square brackets then gives a finite contribution to $u(x)$, which is suppressed relative to $u_1(x)$ by a factor $\frac{m_y}{m_x} \frac{a}{R}$, and hence negligible within continuum description ($\bar{R} \gg a$). The resulting bound-state energy $w_-(x)$ at a given x is thus defined [32] by $u_1(x)$ alone:

$$w_-(x) = -\frac{m_y^*}{2\hbar^2} [u_1(x)]^2 = -\frac{\Delta}{2} \frac{\sin^2\left(\frac{\pi\tilde{x}}{\sqrt{1+\tilde{x}^2}}\right)}{\tilde{x}^2}. \quad (13)$$

It competes with the repulsive contribution of $A^2(x)$:

$$w_+(x) = \frac{A^2(x)}{2m_x} = \frac{\hbar^2}{2m_x R^2} \frac{[\pi/2]^2}{(1 + \tilde{x}^2)^3}. \quad (14)$$

As per Eqs. (5) and (9), \tilde{A}_x^z is odd with respect to y , thus the cross-term $\{\hat{p}_x, \tilde{A}_x^z \sigma^z\} / 2m_x$ averages out upon integration over y . Upon switching to the dimensionless coordinate $\tilde{x} = \frac{x}{R}$, the resulting Hamiltonian $\tilde{\mathcal{H}}_x$ reads

$$\tilde{\mathcal{H}}_x = \frac{\hbar^2}{2m_x R^2} \left[-\frac{d^2}{d\tilde{x}^2} + \frac{[\pi/2]^2}{(1 + \tilde{x}^2)^3} \right] - \frac{\Delta}{2} \frac{\sin^2\left[\frac{\pi\tilde{x}}{\sqrt{1+\tilde{x}^2}}\right]}{\tilde{x}^2}. \quad (15)$$

Taken alone, the last term above is obviously beyond the low-energy approximation. However, with decreasing R , the repulsion grows relative to attraction, and overcomes it at an $\bar{R} \sim \sqrt{\frac{m_y}{m_x}} \sqrt{\xi a} \ll \xi$. Thus Hamiltonian (15) is valid only in a narrow range $R - \bar{R} \ll \bar{R}$, where the bound state becomes shallow to disappear at $R = \bar{R}$. Notice that $\bar{R} \gg a$ as long as the ratio $\frac{m_y}{m_x}$ is not too small ($\frac{m_y}{m_x} \gg \frac{\Delta}{\epsilon_F}$).

Together with Eq. (8), this behavior implies that the Skyrmion-electron bound state defines an ‘optimal’ BP Skyrmion size of the order of ξ . This conclusion can be reached by purely qualitative means, even though quantitative analysis of the problem for $\bar{R} \lesssim R \lesssim \xi$ requires solving Hamiltonian (1) in the presence of the Skyrmion, a task beyond the scope of this work. By particle-hole symmetry, every bound state $\epsilon_0^c(R)$, generated by the conduction band, has a valence-band counterpart $\epsilon_0^v(R) = -\epsilon_0^c(R)$, as shown in Fig. 2. The two states are of the same symmetry, and a crossing of $\epsilon_0^c(R)$ and $\epsilon_0^v(R)$ is ruled out by the general argument that forbids intersection of like symmetry terms in a diatomic molecule [32]. Together with large- and small- R behavior above, this means that $\epsilon_0^c(R)$ must reach its minimum $|\epsilon_0^c(R^*)| \lesssim \Delta$ at an $R^* \sim \xi$, thus defining an ‘optimal’ BP Skyrmion radius, as sketched in Fig. 2 [33].

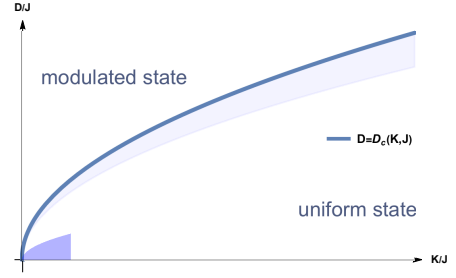


FIG. 3: The parameter space of Eq. (16), represented by D/J and K/J . The boundary $D = D_c(K, J) = \frac{4}{\pi} \sqrt{KJ}$ between the uniform Néel state ($D < D_c(K, J)$) and the modulated phase ($D > D_c(K, J)$) is shown by the solid line. The lightly-shaded area indicates the stability region of the Skyrmion-electron bound state as per inequality (17). The darkly-shaded region near the origin shows the range, where the BP profile is relevant, as defined by conditions (18).

Broader implications — Even for a perfectly centrosymmetric isotropic antiferromagnet, the device substrate induces anisotropy and inversion asymmetry with ensuing single-ion anisotropy and DM coupling [34, 35]. Consider the energy \mathcal{W} of a texture in such a device:

$$\mathcal{W} = \int d^2\mathbf{r} \left\{ J(\nabla \hat{\mathbf{n}})^2 - \frac{K}{a^2} [n_z^2 - 1] + \frac{D}{a} (\hat{\mathbf{n}} \cdot \nabla \times \hat{\mathbf{n}}) \right\}, \quad (16)$$

written as the continuum limit of a spin model on a lattice of spacing a , with stiffness J , single-ion anisotropy K , and DM coupling D . In the ground-state diagram of model (16), a transition line $D = D_c(K, J)$ separates the uniform Néel state at $D < D_c(K, J)$ from a modulated phase at $D > D_c(K, J)$ [36, 37]. At mean field, the transition line is given by $\frac{4}{\pi} D_c(K, J) = \sqrt{JK}$ [36, 37]. At $K = D = 0$, the Skyrmion assumes the BP profile of R -independent energy $\mathcal{W} = 4\pi J$ [6]. With D approaching $D_c(K, J)$ from the uniform state, the Skyrmion evolves into a circular domain wall of radius R_w [38–42]. Concurrently, R_w diverges and \mathcal{W} vanishes continuously, marking the transition to the modulated state [39–41].

The Skyrmion-electron energy consists of the bound-state contribution of the order of Δ [43], and of the magnetic part \mathcal{W} . For Δ small against \mathcal{W} , the Skyrmion remains metastable, yet the bound state modifies its shape and enhances its stability by reducing energy. At the same time, \mathcal{W} (in the absence of the electron) vanishing at the transition to the modulated phase means that, sufficiently close to $D = D_c(K, J)$, one inevitably finds $\Delta \gg \mathcal{W}$. Near $D = D_c(K, J)$, Ref. [40] finds $\mathcal{W} \approx 0.55 \cdot 2^{5/2} \pi^{3/2} J \sqrt{1 - \frac{D}{D_c(K, J)}}$. The condition $\Delta \gtrsim \mathcal{W}$ thus implies

$$1 - \frac{D}{D_c(K, J)} = 1 - \frac{\pi}{4} \frac{D}{\sqrt{JK}} \lesssim \frac{1}{9.8\pi^3} \left(\frac{\Delta}{J} \right)^2. \quad (17)$$

In the range (17), sketched in Fig. 3, it is the bound-state

mechanism that dictates the resulting Skyrmion profile and turns the Skyrmion from a metastable entity into a truly stable one. This is a key result of our work [44].

What is the scope of the BP example ($K = D = 0$) in terms of K and D ? Firstly, the bound-state energy scale Δ must be small against the BP Skyrmion energy $4\pi J$, or the bound state may favor a different profile. Inequality $\Delta \ll 4\pi J$ is favored by the factor 4π in front of J , and by $J \propto S^2$ versus $\Delta \propto S$ scaling with the ordered moment S ; it appears to hold in systems, where estimates have been made [45]. Secondly, it is necessary that the single-ion anisotropy contribution E_a to \mathcal{W} be small against both Δ and $4\pi J$. Eq. (16) shows that $E_a \propto K \left(\frac{R}{a}\right)^2$ [46]. The constraint $E_a \ll \Delta$ must be imposed for the ‘optimal’ $R \sim \xi$, while the relevant condition for D is $D \ll D_c(K, J)$:

$$\frac{K}{\Delta} \ll \left(\frac{\Delta}{\epsilon_F}\right)^2 \quad \text{and} \quad \frac{D}{J} \ll \frac{4}{\pi} \sqrt{\frac{K}{J}}, \quad (18)$$

see Fig. 3. For greater K and D , the solution to the Skyrmion-electron problem must account for the single-ion anisotropy and the DM coupling.

Finally, the condition for treating the Skyrmion profile as static input to the electron problem amounts to the bound-state energy scale Δ being large against that of low-energy localized eigenmodes of the Skyrmion. These are bound from above by the spin wave gap Ω_0 of the bulk magnon spectrum [47]. Thus, the static-Skyrmion approximation holds for $\Omega_0 \ll \Delta$, which also means that the low-energy localized eigenmodes of the Skyrmion are perturbed by the bound electron. In the relevant limit $K \ll J$, the behavior $\Omega_0 \sim \sqrt{KJ}$ [48, 49] translates the condition $\Omega_0 \ll \Delta$ into $\sqrt{KJ} \ll \Delta$ [50]. Outside this range, staggered magnetization $\hat{\mathbf{n}}_{\mathbf{r}}$ and the electron must be treated on an equal footing.

Discussion and conclusions — We have demonstrated the appearance of a Skyrmion-electron bound state in a Néel antiferromagnet with a specific location of the electron band extrema. The bound state does not rely on the BP profile we used as an illustration, and emerges for *any* credible shape such as that of a domain-wall Skyrmion. Similarly, we made use of the mass anisotropy, typical of point Σ , yet the emerging physics picture is qualitatively insensitive to it.

The Skyrmion-electron bound state owes its existence to the texture-induced spin-orbit coupling, the last term in Eq. (4). The latter arises from Néel order, and has no equivalent in a ferromagnet. At the same time, the said term hinges on the lower symmetry of Σ points in the Brillouin zone: at the corner points X or the center point Γ in Fig. 1, such a term is not allowed.

As we have shown, the Skyrmion-electron bound state is nondegenerate, and its energy scale is the gap Δ of the electron spectrum of the Néel state. In this regard, the texture-induced spin-orbit coupling is a real-space

relative of the band splitting effects of the same scale in certain types of collinear antiferromagnets [51–54].

The Skyrmion-electron bound state is a new arrival in the family of electron states, localized on topological defects such as dislocations [55], vortices in superconductors [56] or solitons in organic materials [57, 58]. In addition to its fundamental interest, charged Skyrmion can be manipulated by electric field, which may open new possibilities for its use in devices. We hope that our results stimulate further work both on fundamental and applied aspects of this phenomenon.

We thank P. Pujol for the many discussions, helpful suggestions and enlightening remarks. We are grateful to Ya. Bazaliy for illuminating comments, and to M. Kartsovnik for pointing us to Ref. [45].

* davier@irsamc.ups-tlse.fr

† revaz@irsamc.ups-tlse.fr

- [1] C. Back *et al.*, J. Phys. D: Appl. Phys. **53**, 363001 (2020).
- [2] B. Göbel, I. Mertig, O. A. Tretiakov, Phys. Rep. **895**, 1 (2021).
- [3] P. F. Bessarab, D. Yudin, D. R. Gulevich, P. Wadley, M. Titov, and O. A. Tretiakov, Phys. Rev. B **99**, 140411(R) (2019).
- [4] B. Göbel, A. Mook, J. Henk, and I. Mertig, Phys. Rev. B **96**, 060406(R) (2017).
- [5] A. V. Bezvershenko, A. K. Kolezhuk, and B. A. Ivanov, Phys. Rev. B **97**, 054408 (2018).
- [6] R. Rajaraman, *Solitons and Instantons* (North-Holland, Amsterdam, 1989).
- [7] N. I. Kulikov and V. V. Tugushev, Usp. Fiz. Nauk **144**, 643 (1984) [Sov. Phys. Usp. **27**, 954 (1984)].
- [8] C. Kittel *Quantum Theory of Solids* (John Wiley & Sons, Inc., New York – London, 1963).
- [9] G. E. Volovik, J. Phys. C: Solid State Phys. **20**, L83 (1987).
- [10] V. B. Berestetskii, E. M. Lifshitz and L. P. Pitaevskii, “Course of Theoretical Physics”, Vol. 4, *Quantum Electrodynamics* (Pergamon Press, Oxford, 1982).
- [11] L. H. Ryder, *Quantum Field Theory* (Cambridge University Press, Cambridge, 1996).
- [12] The terms omitted when passing from Eq. (3) to (4) are higher order in momentum. They are negligible as long as the low-energy approximation of Eqs. (3-4) is valid.
- [13] B. I. Shraiman, E. D. Siggia, Phys. Rev. Lett. **62**, 1564 (1989).
- [14] N. P. Armitage, F. Ronning, D. H. Lu, C. Kim, A. Damascelli, K. M. Shen, D. L. Feng, H. Eisaki, Z.-X. Shen, P. K. Mang, N. Kaneko, M. Greven, Y. Onose, Y. Taguchi, and Y. Tokura, Phys. Rev. Lett. **88**, 257001 (2002).
- [15] H. Matsui, T. Takahashi, T. Sato, K. Terashima, H. Ding, T. Uefuji, and K. Yamada, Phys. Rev. B **75**, 224514 (2007).
- [16] D. Song, G. Han, W. Kyung, J. Seo, S. Cho, B. S. Kim, M. Arita, K. Shimada, H. Namatame, M. Taniguchi, Y. Yoshida, H. Eisaki, S. R. Park, and C. Kim, Phys. Rev. Lett. **118**, 137001 (2017).
- [17] G. M. Luke, L. P. Le, B. J. Sternlieb, Y. J. Uemura, J. H.

- Brewer, R. Kadono, R. F. Kiefl, S. R. Kreitzman, T. M. Riseman, C. E. Stronach, M. R. Davis, S. Uchida, H. Takagi, Y. Tokura, Y. Hidaka, T. Murakami, J. Gopalakrishnan, A. W. Sleight, M. A. Subramanian, E. A. Early, J. T. Markert, M. B. Maple, and C. L. Seaman, *Phys. Rev. B* **42**, 7981 (1990).
- [18] E. M. Motoyama, G. Yu, I. M. Vishik, O. P. Vajk, P. K. Mang, and M. Greven, *Nature* **445**, 186 (2007).
- [19] P. K. Mang, S. Larochele, A. Mehta, O. P. Vajk, A. S. Erickson, L. Lu, W. J. L. Buyers, A. F. Marshall, K. Prokes, and M. Greven, *Phys. Rev. B* **70**, 094507 (2004).
- [20] H. Saadaoui, Z. Salman, H. Luetkens, T. Prokscha, A. Suter, W. A. MacFarlane, Y. Jiang, K. Jin, R. L. Greene, E. Morenzoni, and R. F. Kiefl, *Nat. Commun.* **6**, 6041 (2015).
- [21] K. Yamada, K. Kurahashi, T. Uefuji, M. Fujita, S. Park, S.-H. Lee, and Y. Endoh, *Phys. Rev. Lett.* **90**, 137004 (2003).
- [22] H. J. Kang, P. Dai, H. A. Mook, D. N. Argyriou, V. Sikolenko, J. W. Lynn, Y. Kurita, S. Komiya, and Y. Ando, *Phys. Rev. B* **71**, 214512 (2005).
- [23] Y. Dagan, M. C. Barr, W. M. Fisher, R. Beck, T. Dhakal, A. Biswas, and R. L. Greene, *Phys. Rev. Lett.* **94**, 057005 (2005).
- [24] W. Yu, J. S. Higgins, P. Bach, and R. L. Greene, *Phys. Rev. B* **76**, 020503(R) (2007).
- [25] A. Dorantes, A. Alshemi, Z. Huang, A. Erb, T. Helm, and M. V. Kartsovnik, *Phys. Rev. B* **97**, 054430 (2018).
- [26] R. Ramazashvili, P. D. Grigoriev, T. Helm, F. Kollmannsberger, M. Kunz, W. Biberacher, E. Kampert, H. Fujiwara, A. Erb, J. Wosnitza, R. Gross, and M. V. Kartsovnik *npj Quantum Mater.* **6**, 11 (2021).
- [27] G. Tatara, H. Kohno, and J. Shibata, *Phys. Rep.* **468**, 213 (2008).
- [28] This is true for *any* $Q = 1$ Skyrmion profile. For an arbitrary Q , the corresponding flux is $\pm 2\pi Q$.
- [29] The strikingly simple r.h.s. of Eq. (7) is a remarkable property of the BP Skyrmion.
- [30] For chirality $\gamma \neq 0$, spin polarization of the bound state is tilted by γ relative to the local \hat{x} axis in Fig. 1.
- [31] J. C. Tully, Perspective on “Zur Quantentheorie der Molekeln”. In: Cramer C.J., Truhlar D.G. (eds) *Theoretical Chemistry Accounts* (Springer, Berlin, Heidelberg, 2000).
- [32] L. D. Landau and E. M. Lifshitz, “Course of Theoretical Physics”, Vol. 3, *Quantum Mechanics, Non-relativistic Theory* (Pergamon Press, Oxford, 1991).
- [33] By virtue of realizing the energy minimum, such a BP Skyrmion is stable with respect to variation of R . However, finding the optimal Skyrmion shape without restriction to the BP profile, and establishing its stability to any possible deformation is outside the scope of the present work, see Ref. [5] for a comprehensive discussion.
- [34] I. E. Dzyaloshinskii, *Zh. Eksp. Teor. Fiz.* **32**, 1547 (1957) [*Sov. Phys. JETP* **5**, 1259 (1957)].
- [35] T. Moriya, *Phys. Rev.* **120**, 91 (1960).
- [36] A. Bogdanov, A. Hubert, *J. Magn. Magn. Mater.* **138**, 255 (1994).
- [37] A. N. Bogdanov, U. K. Rößler, M. Wolf, and K.-H. Müller, *Phys. Rev. B* **66**, 214410 (2002).
- [38] V. P. Voronov, B. A. Ivanov, and A. M. Kosevich, *Zh. Eksp. Teor. Fiz.* **84**, 2235 (1983) [*Sov. Phys. JETP* **57**, 1303 (1983)].
- [39] X. S. Wang, H. Y. Yuan, and X. R. Wang, *Commun Phys* **1**, 31 (2018).
- [40] S. Komineas, C. Melcher, and S. Venakides, *Physica D* **418**, 132842 (2021).
- [41] H. Jia, B. Zimmermann, M. Hoffmann, M. Sallermann, G. Bihlmayer, and S. Blügel, *Phys. Rev. Materials* **4**, 094407 (2020).
- [42] S. Komineas, C. Melcher, and S. Venakides, *Nonlinearity*, **33**, 3395 (2020).
- [43] Here, we showed this for a BP Skyrmion. Our variational calculation for a domain-wall profile gave the same result.
- [44] Notice that Ref. [3] finds longer Skyrmion lifetimes near the transition line, as well.
- [45] T. Mori and M. Katsuhara, *Journ. Phys. Soc. Japan*, **71**, 826 (2002).
- [46] In this crude estimate, we omit subleading logarithmic enhancement factors [38].
- [47] V. P. Kravchuk, O. Gomonay, D. D. Sheka, D. R. Rodrigues, K. Everschor-Sitte, J. Sinova, J. van den Brink, and Yu. Gaididei, *Phys. Rev. B* **99**, 184429 (2019).
- [48] C. Kittel, *Phys. Rev.* **82**, 565 (1951).
- [49] S. M. Rezende, A. Azevedo, and R. L. Rodríguez-Suárez, *J. Appl. Phys.* **126**, 151101 (2019).
- [50] In the genuine stability range (17), this implies $D \ll \Delta$.
- [51] S. I. Pekar and E. I. Rashba, *Zh. Eksp. Teor. Fiz.* **47**, 1927 (1964) [*Sov. Phys. JETP* **20**, 1295 (1965)].
- [52] S. Hayami, Y. Yanagi, and H. Kusunose, *J. Phys. Soc. Jpn.* **88**, 123702 (2019).
- [53] L.-D. Yuan, Z. Wang, J.-W. Luo, E. I. Rashba, and A. Zunger, *Phys. Rev. B* **102**, 014422 (2020).
- [54] H. Reichlová, R. L. Seeger, R. González-Hernández, I. Kounta, R. Schlitz, D. Krieger, P. Ritzinger, M. Lamme, M. Leiviskä, V. Petríček, P. Doležal, E. Schmoranzarová, A. Bad'ura, A. Thomas, V. Baltz, L. Michez, J. Sinova, S. T. B. Goennenwein, T. Jungwirth, L. Šmejkal, arXiv:2012.15651.
- [55] R. Landauer, *Phys. Rev.* **94**, 1386 (1954).
- [56] C. Caroli, P. G. De Gennes, J. Matricon, *Phys. Lett.* **9**, 307 (1964).
- [57] S. A. Brazovskii and N. N. Kirova, *Sov. Sci. Rev. A* **5**, 99 (1984).
- [58] A. J. Heeger, S. Kivelson, J. R. Schrieffer, and W. -P. Su, *Rev. Mod. Phys.* **60**, 781 (1988).